


External dose reconstruction for the former village of Metlino (Techa River, Russia) based on environmental surveys, luminescence measurements, and radiation transport modelling

M. M. Hiller¹  · C. Woda¹ · N. G. Bougrov² · M. O. Degteva² · O. Ivanov³ · A. Ulanovsky¹ · S. Romanov⁴

Received: 18 November 2016 / Accepted: 5 March 2017
© Springer-Verlag Berlin Heidelberg 2017

Abstract In the first years of its operation, the Mayak Production Association, a facility part of the Soviet nuclear weapons program in the Southern Urals, Russia, discharged large amounts of radioactively contaminated effluent into the nearby Techa River, thus exposing the people living at this river to external and internal radiations. The Techa River Cohort is a cohort intensely studied in epidemiology to investigate the correlation between low-dose radiation and health effects on humans. For the individuals in the cohort, the Techa River Dosimetry System describes the accumulated dose in human organs and tissues. In particular, organ doses from external exposure are derived from estimates of dose rate in air on the Techa River banks which were estimated from measurements and Monte Carlo modelling. Individual doses are calculated in accordance with historical records of individuals' residence histories, observational data of typical lifestyles for different age groups, and age-dependent conversion factors from air kerma to organ dose. The work here describes an experimentally independent assessment of the key input parameter of the dosimetry system, the integral air kerma, for the former village of Metlino, upper Techa River region. The aim of this work was thus to validate the Techa River Dosimetry System for the location of Metlino in an independent approach.

Dose reconstruction based on dose measurements in bricks from a church tower and Monte Carlo calculations was used to model the historic air kerma accumulated in the time from 1949 to 1956 at the shoreline of the Techa River in Metlino. Main issues are caused by a change in the landscape after the evacuation of the village in 1956. Based on measurements and published information and data, two separate models for the historic pre-evacuation geometry and for the current geometry of Metlino were created. Using both models, a value for the air kerma was reconstructed, which agrees with that obtained in the Techa River Dosimetry System within a factor of two.

Keywords Techa River Dosimetry System (TRDS) · Techa River Cohort (TRC) · TL/OSL measurements · Radiation transport calculations · Retrospective dosimetry · Historic dose reconstruction

Introduction

The Mayak Production Association (PA) started to become operational in 1948 near the city of Ozyorsk in the Southern Urals area as part of the Soviet nuclear weapons project (Anspaugh et al. 2002). The main objective of the plant was the production of plutonium for nuclear weapons. For that purpose, several uranium-graphite reactors were created along with other facilities. In the first years of operation, the liquid radioactive waste from the Mayak PA was disposed into the nearby Techa River with variations in the release characteristic. In the following years, a system of reservoir lakes was created to retain the liquid waste (Vorbiova et al. 1999; Mokrov et al. 2000).

As a consequence of the discharges, the inhabitants of the villages along the Techa River were exposed to external

✉ M. M. Hiller
mauritius.hiller@gmx.de

¹ Helmholtz Zentrum München, German Research Center for Environmental Health, Institute of Radiation Protection, 85764 Neuherberg, Germany

² Urals Research Center for Radiation Medicine, Chelyabinsk, Russia

³ Kurchatov Institute Moscow, Moscow 123182, Russia

⁴ Southern Urals Biophysics Institute, Ozyorsk, Russia

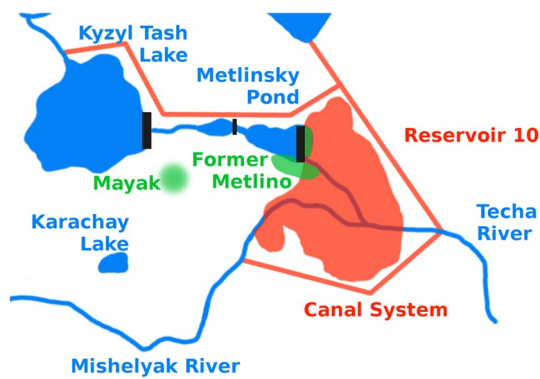


Fig. 1 Upper Techa River in the area of Metlino

and internal radiation. Due to the high radiation, most of the villages along the Techa River were evacuated a few years after the contamination had started. The highest external doses occurred in the former village of Metlino, the village at the Techa River closest to the facilities of Mayak, about 7 km downstream. Metlino was evacuated in 1956. In course of the evacuation, all buildings except for a complex of a mill, a granary, and a church were destroyed. The reservoir number 10 was created on parts of the former village, making it difficult to reconstruct the historic contamination today.

Figure 1 shows the upper part of the hydrologic Techa River system after the evacuation of Metlino (Vorobiova et al. 1999; Mokrov et al. 2000) and Fig. 2 shows the map of Metlino for the time between 1949 and 1951.

Today, the Techa River Cohort (TRC) is among the most studied cohorts for late health effects associated with low-dose rate exposure from intakes of radioactive strontium and caesium as well as external gamma radiation. Individuals in this group suffered from a long-term exposure with lower levels of radiation dose rate, as compared to the individuals in, e.g., the cohorts of the survivors of the atomic bombs (Davis et al. 2015; Krestinina et al. 2013a, b; Schonfeld et al. 2013).

To correlate the health effects to doses, a dosimetry system for the people living along the Techa River, the Techa River Dosimetry System (TRDS), was established (Degteva et al. 2000a, b, 2006). It assesses the external and internal doses to individuals living along the Techa River. The external dose is derived from the dose rate in air along the Techa River banks. Doses to individuals are calculated in accordance with historical records of the residence history, observational data of typical lifestyles for different age groups, and age-dependent conversion factors from air kerma to organ dose.

The assessment of the external dose in the TRDS can be described by the following equation (Degteva et al. 2000a; Taranenko et al. 2003; Ulanovsky et al. 2009, 2010):

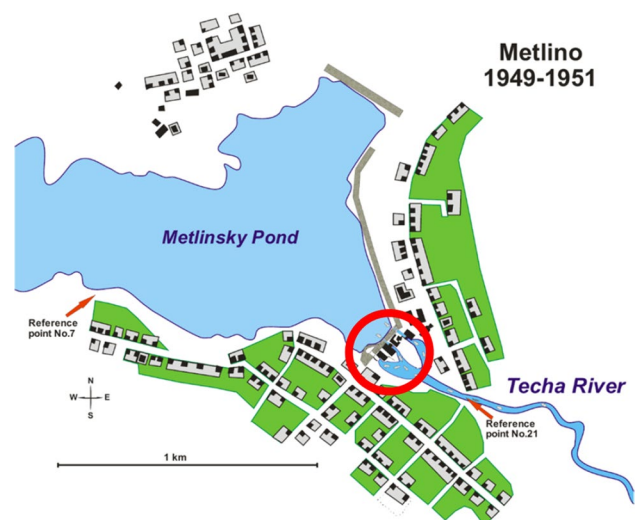


Fig. 2 Village of Metlino before its evacuation. The houses of the village are on both sides of the Metlinsky pond. The center of the map shows the location dam, mill, granary and the church (circle). This area is shown in detail in Fig. 3. Indicated in the map are locations of reference points of the TRDS. The measurements shown in Fig. 10 were performed roughly 100 m downstream the Techa River from the dam, starting at reference point 21 (lower right arrow)

$$D_g = C_g \int_{\Delta T} dt K_r(t) \sum_L \omega_L \tau_L \quad (1)$$

where D_g is the absorbed dose in organ g due to the external exposure in the time period ΔT , g is the organ in the body of the inhabitant, C_g is the organ dose coefficient for organ g , “organ dose per air kerma” (Gy Gy^{-1}), ΔT is the duration of the exposure of the inhabitant (a), $K_r(t)$ is the annual air kerma rate in the settlement 1 m above the shoreline (Gy a^{-1}), r is the distance from Mayak PA along the Techa River, L is a set of locations where the inhabitant spent his/her time, ω_L are air kerma reduction factors for the locations L relative to the shoreline air kerma, and τ_L are time fractions of ΔT , spent at the location L by the inhabitant of the village (a).

For the accurate correlation of health effects observed in members of this cohort with a dose received by the individual, continuous improvements in dosimetry and validation by independent methods are necessary. The evaluation presented here is in the environmental module of the TRDS: using experimental input data and radiation transport calculations, the air kerma at the shoreline, accumulated from the beginning of the contamination in 1949 to the evacuation of the village in 1956, K_x , can be assessed and compared with the TRDS estimate, derived from integrating the time-dependent air kerma rate at the shoreline, $K_r(t)$:

$$K_x = \int_{1949}^{1956} K_r(t) dt \quad (2)$$

In this work, Monte Carlo calculations are employed for a historic dose reconstruction and assessment. These calculations are based on the results of recent luminescence measurements (Woda et al. (in prep.)). In these measurements, the church tower serves as a new dose archive that offers the possibility of an independent study based on current, precise experimental data, not historic measurements. The usability of bricks as a solid-state dosimeter using either Thermoluminescence (TL) or Optically Stimulated Luminescence (OSL) has been shown in earlier Techa River studies (Bougrov et al. 1998, 2002; Göksu et al. 2002; Woda et al. 2009, 2011). The dose estimated using the bricks is the integral dose of the total exposure of the brick. Results of those TL/OSL measurements were combined with those of environmental dose rate and other measurements in this study. With this approach, an independent assessment of external doses for the village of Metlino can be achieved, not using any input parameters of the TRDS. Depending on the outcome, the results obtained in the present study can either add to the confidence in the TRDS for this site or open a discussion on the validity of the TRDS for Metlino.

It should be noted that an external dose assessment for Metlino was already performed in two earlier studies (Jacob et al. 2003; Taranenko et al. 2003; Degteva et al. 2015b). The investigations performed in these earlier works were based on the coupled application of luminescence measurement of bricks sampled from the southwestern wall of the former mill (see Fig. 3) and radiation transport modelling. However, it was revealed later that the assumptions on the source term used in Jacob et al. (2003) and Taranenko et al. (2003) for the radiation transport modelling were not correct, and the history of the radioactive contamination was reconstructed in more detail (Degteva et al. 2012; Shagina et al. 2012). In addition, it was revealed that the path of the Techa River through the village of Metlino and consequently the assumed geometry of the contaminated floodplains at the shores of the Techa River were different from the data set available in 2003 (Mokrov et al. 2005). Taranenko et al. (2013) verified the external dose in Metlino using the southwestern wall of the mill as a dose archive, and the new data on the source term and the historic changes in the exposure geometry (Fig. 3). However, it became clear that it would be useful to investigate the possibility of other buildings to serve as a dose archive. Because all of the walls of the granary, except the northwestern wall not facing the Techa River, have collapsed in the past 10–20 years, the church tower comes into focus

and is mainly investigated in this work. The church tower is adjacent to the eastern arm of the Techa River (Fig. 3) and faces towards several directions of interest. A feasibility study to use the church tower as a dose archive was performed previously (Degteva et al. 2008), but a full-scale validation study using this building was still lacking.

The present work is part of the project SOLO (epidemiological studies of exposed populations in the Southern Urals), funded by the European Union. The scope of the SOLO project comprised epidemiological studies of exposed Southern Urals populations and an improved assessment of the correlated dose. Next to the approach to reconstruct the dose for the location of Metlino described here, two other experimental methods used for validation of dosimetry systems were employed in SOLO: electron paramagnetic resonance (EPR) and fluorescence in situ hybridization (FISH) measurements were used for the dose assessment for inhabitants of villages along the Techa River (Degteva et al. 2015a; Shishkina et al. 2016; Vozilova et al. 2012).

Materials and methods

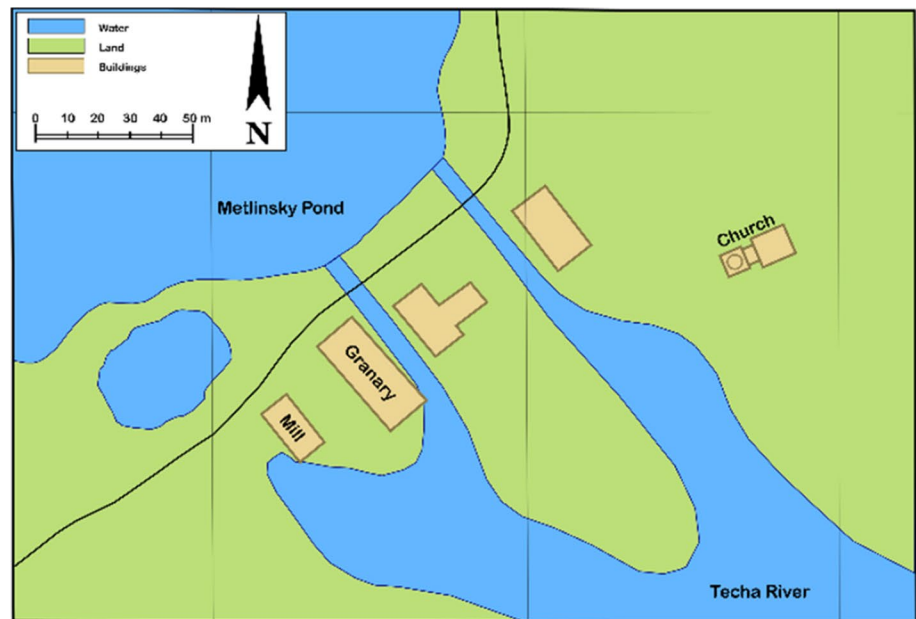
Description of the Metlino area before evacuation and today

The landscape in Metlino has changed significantly between the time when the village was inhabited and the time after the evacuation. For the time before the evacuation (historic Metlino), houses were located on both sides of the Techa River and around the Metlinsky pond (Fig. 2). A dam was holding back the Metlinsky pond with the complex of a mill and a granary just after it. The Techa River was flowing out of the Metlinsky pond in two arms leaving a small peninsula between them. A third arm formed a blind creek behind the mill and the granary. The church was to the east of the Techa River, at a distance of about 20–25 m.

After the evacuation in 1956, the landscape was transformed in a few consecutive steps until it reached the shape which it still has today (current Metlino site). The dam was reinforced, increased in height and the area between the mill and the church was flooded, starting to become the reservoir number 10. The area comprising the contaminated floodplains and shorelines is now shielded by several meters of water. The reservoir today reaches almost up to the church. The remaining area surrounding the church is frequently flooded with water from the reservoir and is an open boggy contaminated terrain.

One of the main issues in the dose reconstruction presented here is the change in exposure geometry

Fig. 3 Historic (a) and current (b) geometry of the village of Metlino. **a** Drawn after a recently declassified map shown in Fig. 5. **b** Drawn after current Google Maps data. In the historic scenario, the Techa River was flowing out of the Metlinsky pond in two arms, whilst in the current situation, the outlet of the Metlinsky pond to the reservoir number 10 is controlled by a weir



(a)



(b)

introduced by the change in landscape. Measurements can only be performed on the current geometry, but the final aim is to derive an air kerma value for the historic geometry.

Sampling and luminescence measurements

The church tower was selected as a dose archive for sampling and luminescence measurements. Brick samples were collected for TL/OSL measurements to determine the total accumulated dose, and thermoluminescent dosimeters

based on $\text{Al}_2\text{O}_3:\text{C}$ (TLD-500) were inserted at selected sampling locations to determine the seasonally averaged annual dose accumulated nowadays. Only the basic sampling strategy and measurement results are reported here. For details concerning measurements and employed methodologies, the reader is referred to Woda et al. (in prep.).

For sample collection and environmental measurements, three field trips were performed to Metlino in 2011, 2012, and 2013. Selected measurement results from a field trip in 2008, carried out in the framework of the Southern Urals

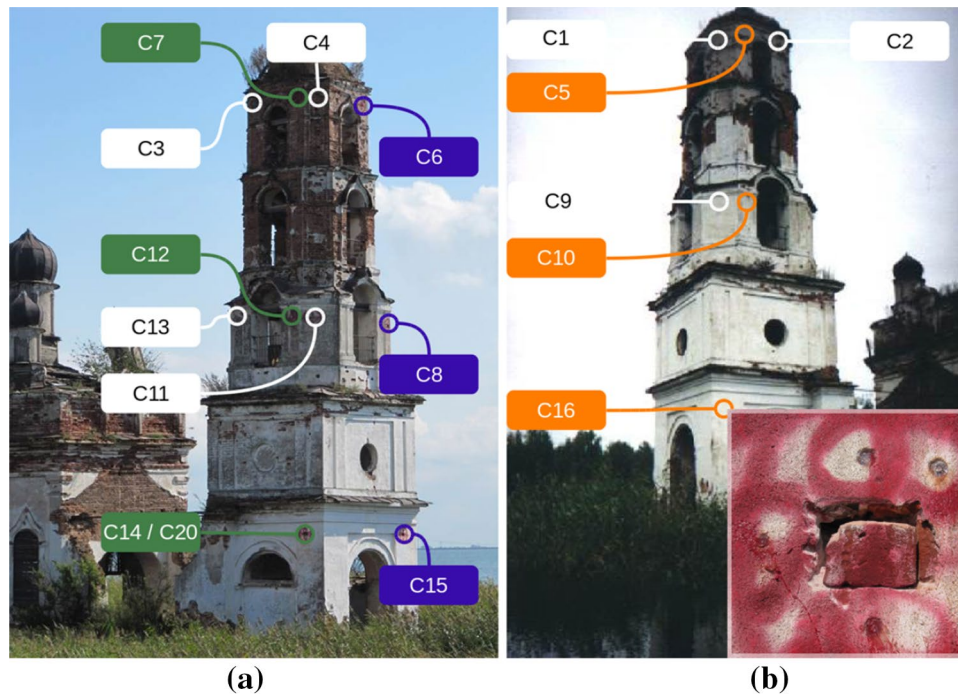


Fig. 4 Church tower from two different sides. The tower has five stories with the lower two having rectangular structures, the upper three having octagonal structures. All sites where brick samples were retrieved or TLD samples were installed are marked. **a** Northern walls of the church tower; **b** southern walls. Sampling sites C14/C20, C12, and C7, taken from the NNW wall are marked in *green*. Sampling sites C15, C8, and C6 were taken from the WSW wall and are shown in *blue*. Sampling sites C16, C10, and C5 taken from the SSE

wall are shown in *orange*. There are several sampling sites on intermittent walls in the octagonal stories, they are marked in *white*: C2, C3, C4, C9, C13, C11, and C1. The *inset* in the lower right corner shows exemplary one of the sampling sites; in the center is a brick sample that is supposed to be extracted. Around the brick sample, the four bore holes can be seen, in which TLD dosimeters were inserted. Those TLD dosimeters were retrieved after 1 year. (Color figure online)

Radiation Risk Research (SOUL) project, were used as well.

The church tower has five levels, the lower two have a rectangular structure and samples were taken from three walls (Fig. 4):

1. The north–northwestern (NNW) wall, samples C14/C20, C12, and C7. This wall faces towards the swampy area to the north of the church tower.
2. The west–southwestern (WSW) wall, samples C15, C8, C6, and the
3. south–southeastern (SSE) wall, samples C16, C10, and C5. Both are facing towards the former bed of the Techa River.

In the upper levels, the church tower has an octagonal structure, and consequently, samples were taken also from the walls in-between. Samples were taken from three different heights per wall: 3.6, 11.8, and 19.6 m. An overview of the samples taken can be seen in Table 1. Brick samples were analyzed at a depth of 1 cm (0.5–1.5 cm) and 3 cm (2.5–3.5 cm), as measured from the surface of the

wall. At selected locations, they were also analyzed at 5, 7, and 9 cm depth. Quartz grains in the grain size fraction of 140–200 μm were extracted from the brick slices for dose measurements.

The height profile of the dose along each wall gives information about the source distribution in the vicinity of the church tower, helping to experimentally constrain the possible source configuration. The dose–depth profile in the brick can give information about the source energy (ICRU Report 68 2002). Table 1 lists the results of the OSL measurements of the brick samples. The given values are the total anthropogenic dose accumulated in brick since the beginning of the contamination in 1949. The doses were background corrected (Woda et al. in prep).

In addition to the measurements in brick, the external gamma dose rate at the brick sample position was monitored using TLD ($\text{Al}_2\text{O}_3:\text{C}$ dosimeters), stored for 1 year. At each location, three TLD in 3 mm-thick housings made of Al- and one in a 1 mm-thick housing made of Cu were inserted into the wall. As it is shown in Ulanovsky et al. (in prep.), the dose response of the Al-shielded TLD corresponds more to the dose response of the brick

Table 1 Overview of the sampling sites at the church tower

Wall	Height (m)	Sample no.	TL/OSL measurement		TLD measurement	
			Depth (mm)	Dose (mGy)	Dose (mGy a ⁻¹)	
North–northeastern (NNE)	11.8	C13	10 ± 5	647 ± 37		
			30 ± 5	437 ± 29		
			50 ± 5	320 ± 22		
	19.6	C3	15 ± 5	481 ± 33		
			26 ± 5	361 ± 29		
North–northwestern (NNW)	3.6	C14	10 ± 5	2142 ± 146	12.23 ± 0.26	
			30 ± 5	1646 ± 82		
			C20 ^a	10 ± 5	2622 ± 124	
				30 ± 5	1913 ± 89	
		11.8	C12	10 ± 5	968 ± 48	6.49 ± 0.24
West–northwestern (WNW)	19.6	C7	10 ± 5	798 ± 47	5.10 ± 0.20	
			30 ± 5	547 ± 39		
	11.8	C11	10 ± 5	1133 ± 50	5.08 ± 0.24	
			30 ± 5	805 ± 39		
			50 ± 5	558 ± 29		
19.6	C4	15 ± 5	614 ± 36			
		27 ± 5	599 ± 37			
West–southwestern (WSW)	3.6	C15	10 ± 5	866 ± 45	3.32 ± 0.09	
			30 ± 5	601 ± 36		
			50 ± 5	430 ± 27		
	11.8	C8	10 ± 5	982 ± 49	2.47 ± 0.39	
			30 ± 5	670 ± 38		
			50 ± 5	511 ± 33		
19.6	C6	10 ± 5	888 ± 42	2.13 ± 0.57		
		30 ± 5	604 ± 33			
		50 ± 5	436 ± 27			
		70 ± 5	286 ± 23			
South–southwestern (SSW)	11.8	C9	10 ± 5	822 ± 96		
			30 ± 5	677 ± 85		
			50 ± 5	459 ± 45		
	19.6	C1	10 ± 5	825 ± 48		
			21 ± 5	690 ± 44		
South–southeastern (SSE)	3.6	C16	10 ± 5	1240 ± 55	2.75 ± 0.14	
			30 ± 5	813 ± 40		
			50 ± 5	584 ± 34		
	11.8	C10 ^b	10 ± 5	1021 ± 57	1.65 ± 0.47	
			30 ± 5	732 ± 51		
			50 ± 5	545 ± 36		
19.6	C5	10 ± 5	1131 ± 51	1.42 ± 0.26		
		30 ± 5	782 ± 40			
		50 ± 5	582 ± 33			
		70 ± 5	450 ± 30			
		90 ± 5	325 ± 27			
East–southeastern (ESE)	19.6	C2	12 ± 5	801 ± 47		
			20 ± 5	634 ± 41		

For each site, the facing direction of the wall and the height of the sample taken are indicated

The accumulated dose in brick (1949–2012) as measured by luminescence methods is shown for each sample

In addition, the current annual dose as measured in TLD and averaged among the three Al-shielded dosimeters used is shown

^aSample C20 shares the location with C14 (1 brick apart) the TLD; therefore, the values for C14 are also taken for C20

^bFor sample C10, the TL dose values are reported, see Woda et al. (in prep.) for details

than the Cu- shielded TLD, making it favorable to use the Al-shielded TLD for the comparison with brick measurements. Results for the current annual dose estimated by TLD are shown in Table 1. The values were averaged using three Al-shielded TLD at each location.

Environmental measurements

Measurements on reservoir number 10

Environmental measurements were performed on the area of the old Metlino that is now covered by reservoir number 10. During the 2012 field trip, the region of interest was crossed on four transects by boat, starting at the shoreline near the church tower (Fig. 5). Every few meters along the transects, a probe head was lowered to the ground of the lake. The depth of the lake and the activity of the bottom sediment were measured with a collimated in situ gamma spectrometer (Ivanov et al. 2013). From the ratio of the photo peak to the Compton continuum, the surface activity and the thickness of the contaminated layer were determined. The situation in Metlino was not optimal with regard to detector calibration. Therefore, the absolute values of the activity were attributed with a large error of around a factor 2. Yet, the magnitude of the surface activity of about 1 GBq m^{-2} seems reliable, as is the trend of the measurement along the transects. From this trend, conclusions on the location of the arms of the Techa River, the contaminated floodplains, and on relative variations in the contamination levels were drawn; absolute values were not

employed (Potapov et al. 2006). The results of the measurements can be seen in Fig. 6.

Transect 2 (Fig. 5) shows a water depth of about -2 m with a decrease to about -3 m at distances 40 and 70 m from the start. The first decrease shows the first arm of the Techa River, and the second decrease the second arm and also the blind creek. Transects 3 and 4 show the first arm, while the second arm and the blind creek are joint together. The river bed is a little narrower in transect 4 than in transect 3. For transect 4, about 50 m away from transect 2, the peninsula has less elevation. All these observations match the historic map (Fig. 5).

In general, the bottom sediment activity is at the order of 1 GBq m^{-2} across the lake. The increased elevation in the ground level at 70–80 m for transect 2 is in superposition with a decrease in activity to 0.01 GBq m^{-2} . This drop in bottom sediment activity is supported by three separate measurements over a distance of 12 m. It thus can be considered as real. In contrast, similar decreases in activity seen in transects 1 and 3 are indicated by single point measurements only. Considering the comparatively small field of view of the collimated detector, it cannot be excluded that these results are caused by shielding effects due to possible debris on the riverbed and thus are not considered a true measure of the sediment activity. Therefore, these data points were not considered in later analysis. For transect 4, there is a constant activity across the transect, even at the location of the peninsula.

Dose rate mapping around the church tower

The present contamination of the soil in the surrounding of the church tower was assessed by measuring the dose rate in air, 1 m above ground on a $5 \times 5 \text{ m}$ grid, extending up to 50 m distance from the church tower (Fig. 7). Local deviations from the grid were made whenever terrain structure made it necessary. Dose rate measurements were performed in 2012 and repeated in parts in 2013, some parts of the area were also measured in 2008; the general pattern of the dose rate is consistent for the different years. The 2012 measurement was the most precise and extensive and was used in the following calculations. For the measurements, an Automess 6150 AD dose rate meter (Automation und Messtechnik GmbH, Ladenburg, Germany) was employed. The dose rate meter was calibrated for measurement of the ambient dose equivalent rate \dot{H}^* in units of $\mu\text{Sv h}^{-1}$. To convert the meter readings to air kerma rate ($\mu\text{Gy h}^{-1}$), the energy and angular dependence of the detector were determined experimentally in the Secondary Standard Dosimetry Laboratory at the Helmholtz Center Munich and folded with calculated photon spectra for ^{137}Cs distributed in soil.

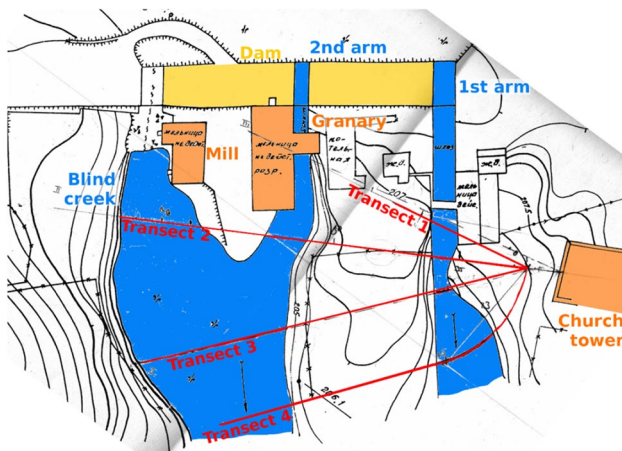


Fig. 5 Recently, declassified map is shown that depicts the Techa River system crossing the village of Metlino in the years before the evacuation (Mokrov et al. 2005). The dam holding back the Metlinsky pond is on the top, with the buildings of the old mill and granary, the new mill, and some support buildings underneath it. The church is shown to the right

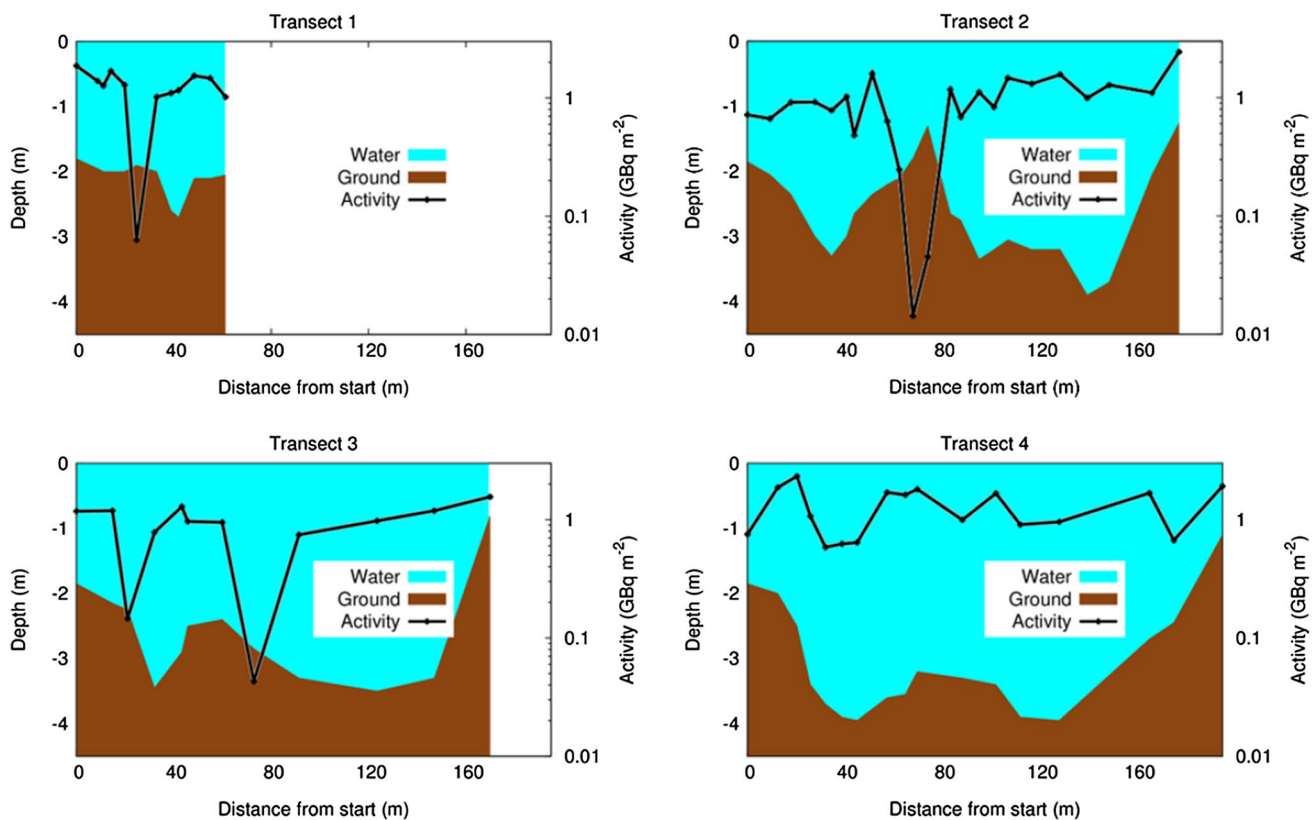


Fig. 6 Reservoir number 10 was crossed by boat along four transects, starting at the shoreline next to the church tower. Every few meters along each transect, the depth of the reservoir was measured and

the activity of the bottom sediment was determined using an in situ gamma spectrometer

This resulted in a conversion coefficient of $\dot{H}^*(10)$ to K_{air} of 0.78.

The north of the church tower is a swampy area; the landscape is flat in this region. To the south of the church tower, there is a strong decline in the elevation profile, and after a few meters distance from the church tower, the reservoir starts. Measurements were performed up to a water depth of approx. 70 cm.

In situ gamma spectrometric measurements in front of the granary

In situ gamma spectrometric measurements were performed in the area in front of the granary in 2008. A depth profile of the activity distribution of ^{137}Cs in soil was measured for two samples. Both measurements show that the majority of the contamination is within the first 30 cm of the soil (Fig. 8). It is assumed that the results of these measurements are also true in the area in front of the belfry as there is only a small distance between the buildings with no notable change in the structure of the soil.

Analysis of historical data

Measurements of the ^{137}Cs concentration in the reservoir number 10

For the dose assessment over the 60 years since the contamination, the estimation of the effective half-life (T_{eff}) of ^{137}Cs is important. The effective half-life does not only account for the physical half-life but also for environmental factors such as migration in ground or sedimentation (Jacob et al. 1997, 2009). Measurements of the ^{137}Cs concentration in the reservoir number 10 were used to determine its effective half-life.

In an earlier study, the effective half-life for the location of Metlino was determined by fitting an exponential decay function to measurements of the specific activity of ^{137}Cs in the water of reservoir number 10 that were made between 1956 and 1997 (Taranenko et al. 2003). Taranenko et al. 2003 estimated a triangular shaped distribution for the effective half-life with a mode of 21.2 a and a minimum and maximum of 12.3 and 30.1 a, respectively. In the present study, this data set was updated with additional data from the URCRM archive and the analysis was repeated.

A linear function was fitted to the logarithm of the activity values, as an exponential fit to the actual measured values would give a higher weight to larger values and lower weight to lower values, which for this data set is not justified. As it can be seen in Fig. 9, the data points show a large scatter, resulting in a considerable uncertainty on the effective half-life, estimating it to $T_{\text{eff}} = 19.5 \pm 5.1 a$. This value agrees within uncertainty limits with the value derived in Taranenko et al. 2003.

Dose rate measurements at shoreline from 1951 to 1954

Measurements of the dose rate in air, 100 m downstream of the dam, for different distances to the shoreline were performed between 1951 and 1954 (Shagina et al. 2012). These measurements show a decreasing dose rate in air with the distance from the shoreline (Fig. 10). The location of the measurements in the village of Metlino is shown in Fig. 2. A double exponential decay function was fit to the data. With this function, ratios of the relative dose rate at the shoreline to the relative dose rate at 10 and 20 m in distance from the shoreline, over the floodplain, were estimated:

$$R_1 = \frac{\text{Relative dose rate in air at the shoreline}}{\text{Relative dose rate in air in 10 m distance from the shoreline}} = 6.2$$

and

$$R_2 = \frac{\text{Relative dose rate in air at the shoreline}}{\text{Relative dose rate in air in 20 m distance from the shoreline}} = 17.5$$

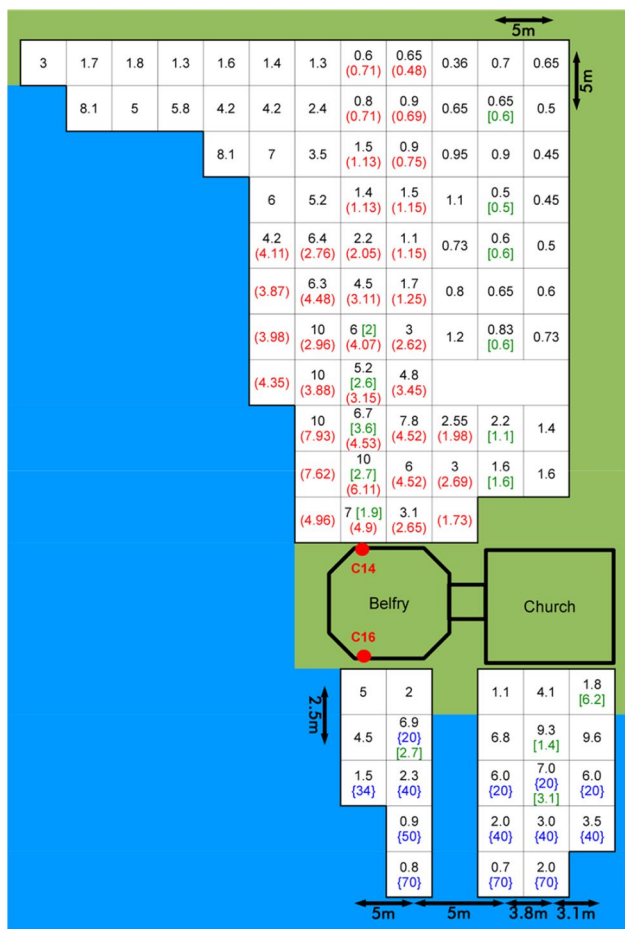


Fig. 7 Dose rates ($\mu\text{Gy h}^{-1}$) in the area to the north and the south of the church tower measured 1 m over ground on a grid with roughly 5 m side length; one white box in the figure depicts one of the cells of the grid. Black numbers 2012 field trip; green numbers enclosed in square brackets—2008 field trip; red numbers enclosed in round brackets—2013 trip; blue numbers enclosed in flower brackets—approximate water depth in centimeter in reservoir number 10 in 2012. (Color figure online)

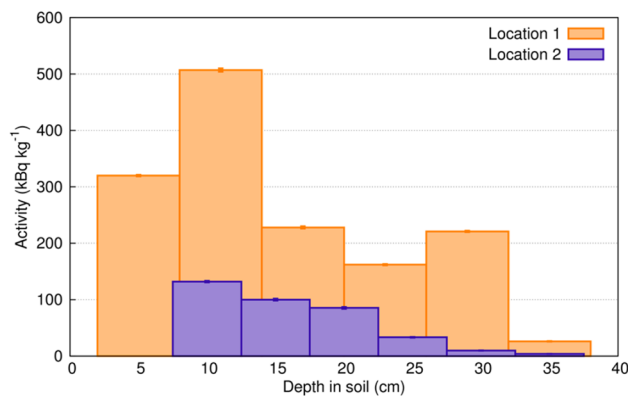


Fig. 8 Depth distribution of the ^{137}Cs activity in soil estimated for two locations in front of the granary

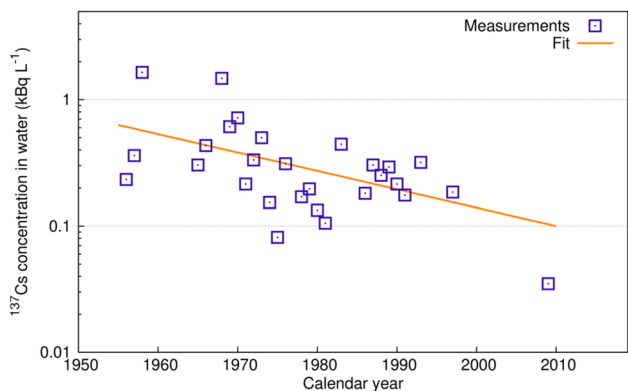


Fig. 9 Measured specific activity of ^{137}Cs in the water of reservoir number 10. Straight line fits to the logarithm of the activity values for estimation of the effective half-life T_{eff}

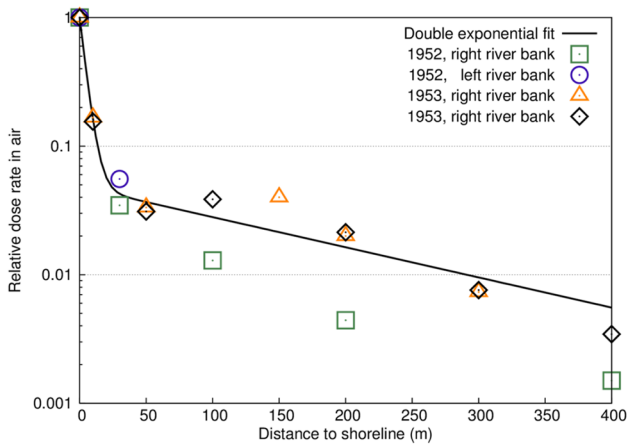


Fig. 10 Relative dose rate in air as a function of the distance to the shoreline, as measured in 1952 and 1953 on the left and the right river bank. Dose rates are normalized to their respective value at 0 m distance. The location of the measurements is indicated in Fig. 2 (Shagina et al. 2012)

Models for radiation transport calculation

Overview

A summary of the methods and the sequence of steps performed to derive the air kerma at shoreline from measurements and simulations at the church tower and its surrounding can be seen in Fig. 11.

Monte Carlo simulations

For the Monte Carlo Calculations, the Monte Carlo-N Particle transport code (MCNP), version 5, 1.60 was used (X-5

Monte Carlo Team 2008). For the dose estimation, the F6 track length estimation tally was employed. The runs were performed until the estimated tally precision was in the order of 3% or lower.

Air and soil were simulated according to Eckerman and Ryman 1993. The composition and density of a brick sample from Metlino were taken from Taranenko et al. 2003. A standard plaster was assumed (Karsten 1997). Table 2 lists the composition and densities of the materials.

Model of the church tower

A detailed model of the church tower was created for the use in the Monte Carlo calculations. The church tower is about 22 m high and has five stories. The lower two stories have a rectangular structure and the top three stories have an octagonal shape. For each story, the inner and outer dimensions, the width of the wall, the location and the dimensions of the windows, and the height of the rooms were measured. The measurements were performed in great detail using a laser range meter (LE200, Stabila GmbH, Trifels, Germany).

The walls of the church tower were covered with a variable amount of plaster between 1.5 and 2 cm. To address the absorption of gamma radiation due to the plaster covering the walls, Monte Carlo calculations were performed to assess a reduction factor P , defined as the ratio of dose in the first cm of brick with plaster layer to the dose in the first cm without plaster. A brick wall was simulated to be covered with an amount of 0–5 cm of plaster. A ^{137}Cs source in soil was simulated in the ground and the spectrum of the source in several heights up to 100 m above ground was recorded. This spectrum was taken as source

Fig. 11 Approach to calculate the integral air kerma at shoreline for the time before the evacuation combining measurements and two models

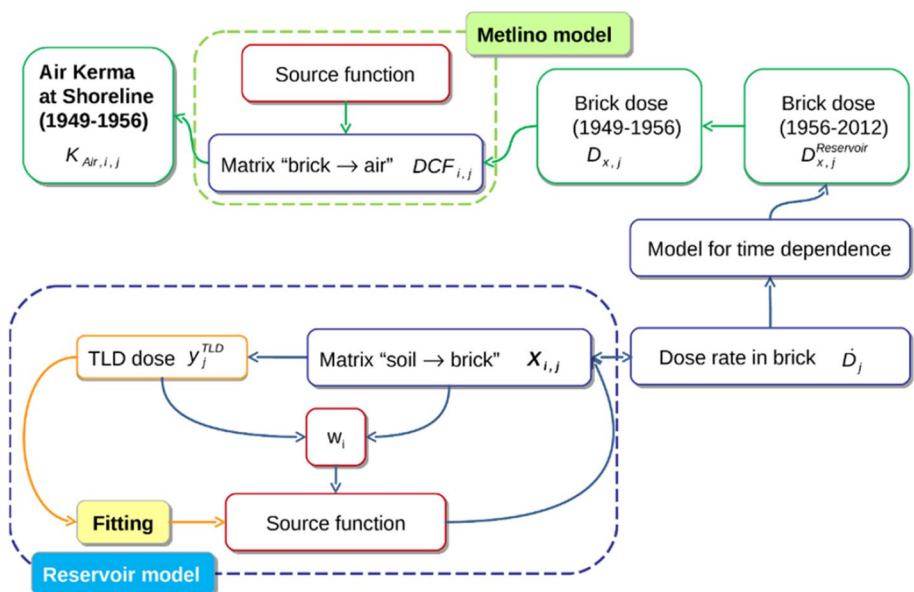


Table 2 Composition of materials used in the MCNP simulation in weight fractions

Element	Z	Weight fraction			
		Air	Soil	Brick	Plaster
H	1	0.001	0.0021		0.0071
C	6	<0.001	0.016		
N	7	0.751			
O	8	0.236	0.577	0.475	0.5063
Na	11			0.005	
Mg	12			0.017	
Al	13		0.050	0.085	
Si	14		0.271	0.296	0.3457
S	16			0.002	
Ar	18	0.013			
K	19		0.013	0.026	
Ca	20			0.040	0.1409
Ti	22			0.006	
Fe	26		0.011	0.048	
Density (g cm ⁻³)		0.00125	1.6	1.8	2

Air and soil are taken from Eckerman and Ryman (1993). A brick sample taken from Metlino was analyzed in Taranenko et al. (2003), and similar values are taken here. The plaster composition is taken from Karsten (1997)

to assess the absorption due to the plaster relative to the height above ground (Fig. 12).

The exact locations of the samples taken for TL/OSL measurements were included in the model of the church tower. At each sampling site, the dose in brick was calculated in ten subsequent, 1 cm-thick sections at a distance of 1–10 cm from the brick surface.

Model of the current site at Metlino—“reservoir model”

The surrounding of the church tower, as it is currently found in Metlino, was implemented as a model for Monte

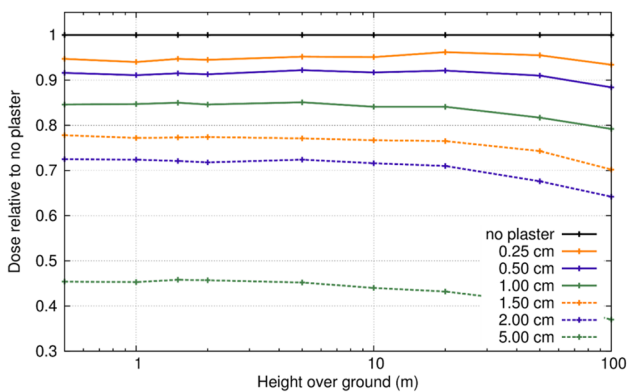


Fig. 12 Relative dose in 1 cm depth in the brick of a wall with no plaster compared to the wall with plaster for plaster with a thickness of 0–5 cm and heights between 0 and 100 m over the ground

Carlo calculations. The reconstruction of the landscape around the church tower was based on a simplification of a Google earth image of the area.

The depth of the source was determined using the in situ gamma spectrometric measurements shown above (refer to Fig. 7). In addition, a formula developed by Minenko et al. 2006 was used to assess the activity $A(z, t)$ with a mass per unit area z (g cm⁻²) at time t after contamination:

$$A(z, t) = A(0, 0) \exp \left\{ -\frac{z}{\beta(t)} \right\} \tag{3}$$

where $\beta(t)$ is called the relaxation mass per unit area (g cm⁻²).

The depth distribution of the activity is shown for times between 0 and 60 years in Fig. 13. Both the measurements and Eq. (3) indicate a distribution of the contamination of up to about 30–40 cm in the relevant time range (50–60 years). Figures 8 and 13 point to a decreasing contamination profile with depth or with a maximum concentration around 10 cm. Measurements on extracted sediment cores from the area north-west to the mill show both, cores with a maximum concentration in the topmost

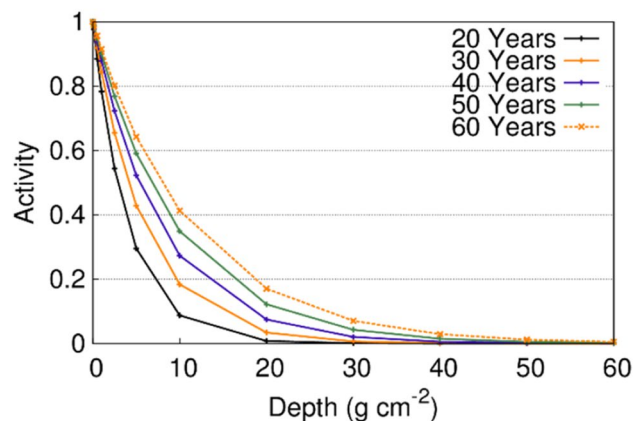
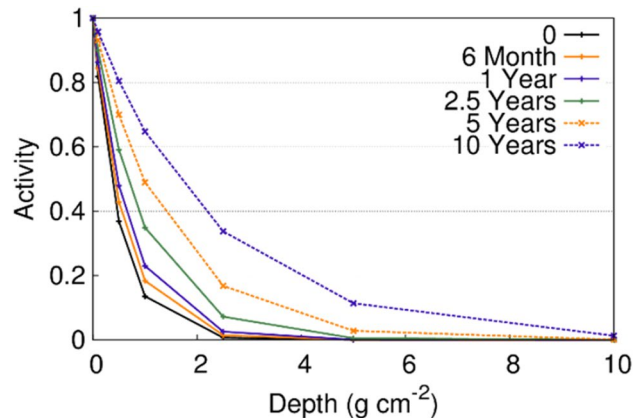


Fig. 13 Estimated depth distribution of radionuclides in soil for 0–60 years, normalized to the surface activity

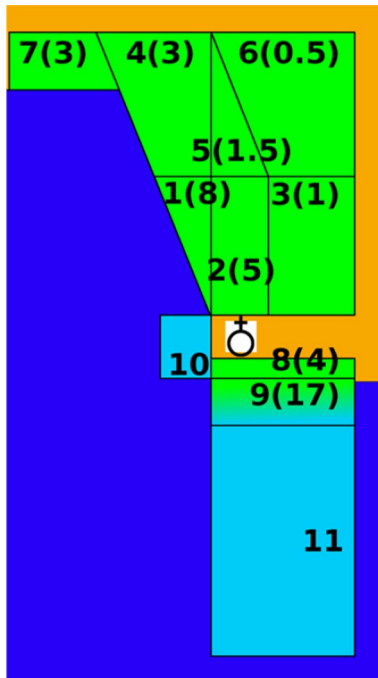


Fig. 14 Model of the current site in Metlino shows the geometry of the surrounding of the church tower. The number of the source is given in *black*. The average measured dose rate for sources 1–9 in $\mu\text{G h}^{-1}$ is shown in *brackets* (). No measurements were performed in sections 10 and 11. Sources 1–8 are in soil (*green areas*), sources 9–11 in the bottom sediment, covered by water (*light blue*). Uncontaminated soil is shown in yellow, water in dark blue. The church tower is in the center white location of the image. (Color figure online)

layer (0–10 cm) and at 30–40 cm (Bougrov et al. 2002). Since the exact shape of the depth distribution of contamination in the relevant area around the church is not known, the simplest case of a homogeneous distribution up to a depth of 30 cm was implemented in the model.

The source regions i were identified based on the dose rate mapping performed in the vicinity of the church tower (Fig. 14). The area was segmented into nine sections with similar dose rate and an average dose rate DR_i was estimated for each section. The relative source strength w_i was determined as.

$$w_i = \frac{\text{DR}_i}{\sum_{i=1}^9 \text{DR}_i} \quad (4)$$

The area to the north of the church tower is a swamp, the landscape is flat. To the south of the church tower, there is a strong decline in the elevation profile, and after a few meter distance from the church tower, the reservoir number 10 starts; the area was divided into a source section above the water level and a section below.

In the first Monte Carlo calculations, with the aim of matching calculated dose rate with measured TLD dose

rates in the wall of the church tower, it was found that the nine source regions were not sufficient to correctly reconstruct the different measured height profiles. As described above, the mapping of the dose rate in the vicinity of the church tower (see Fig. 7) could mainly be performed on land only. Hardly, any measurements were possible over Reservoir 10. Therefore, no measurements were conducted on the west of the church tower and only a few to its south. However, it is not reasonable to assume that the contamination stops at the border of measurement. Therefore, two additional source regions (10, 11) were implemented in the area that was not assessed in the dose rate mapping.

Having identified the source regions, the annual dose at the time of measurement (year 2012) was reconstructed using the reservoir model in combination with the TLD measurements. First, the activity of the sources was determined. For this, the dose in detector j of the church tower due to source i in the ground, x_{ij} , was used to calculate an annual dose in the detector using the reservoir model. This contribution was fitted to the measured annual dose derived from the TLD measurements, \dot{D}_j^{2012} (Table 1).

To increase the robustness of the fitting procedure, the contribution of the first nine sources was added, weighting them with the relative source strength w_i :

$$\sum_{i=1}^9 (x_{ij} \cdot w_i) = x_{1-9,j} \quad (5)$$

Similarly, the activity of sources 1–9 was combined to A_{1-9} , as a sum weighted by the volumes of the sources V_i , with the total volume, $V = \sum_{i=1}^9 V_i$:

$$A_{1-9} = \sum_{i=1}^9 A_i \frac{V_i}{V} \quad (6)$$

The now reduced set of three free parameters, A_{1-9}, A_{10} , and A_{11} (activities of combined source 1–9, and those of sources 10 and 11) were then determined in the fitting process against the annual dose derived using TLD:

$$\begin{pmatrix} x_{1-9,1} & x_{10,1} & x_{11,1} \\ \vdots & \vdots & \vdots \\ x_{1-9,10} & x_{10,10} & x_{11,10} \end{pmatrix} \cdot \begin{pmatrix} A_{1-9} \\ A_{10} \\ A_{11} \end{pmatrix} = \begin{pmatrix} \dot{D}_1^{2012} \\ \vdots \\ \dot{D}_{10}^{2012} \end{pmatrix} \quad (7)$$

In the next step, the dose in brick for the time after the evacuation, $D_{Xj}^{\text{Reservoir}}$, was calculated:

$$D_{Xj}^{\text{Reservoir}} = \int_{1956}^{2012} \dot{D}_j^{2012} \frac{P}{\text{CF}} e^{\frac{\ln(2)}{T_{\text{eff}}}(t-1956)} dt \quad (8)$$

where P is the reduction of the dose in brick by a layer of plaster on the brick wall, and CF is the conversion factor between a dose accumulated in the brick due to a source in

ground in front of the church tower compared to the dose registered in TLD due to the same source.

The plaster on the wall has an average thickness of 1.5–2 cm, samples were taken from heights between 3.6 and 19.6 m. Using Monte Carlo calculations, a reduction of $P = 0.75 \pm 0.025$ was calculated. The conversion factor CF was determined as 0.82 ± 0.08 (Ulanovsky et al. (in prep.)).

Knowing $D_{X,j}^{\text{Reservoir}}$, together with the total dose in brick, $D_{X,j}^{\text{Total}}$, the brick dose for the time before the evacuation, $D_{X,j}$, was calculated:

$$D_{X,j} = D_{X,j}^{\text{Total}} - D_{X,j}^{\text{Reservoir}} \tag{9}$$

Model of the historic site in Metlino—“Metlino model”

To be able to reconstruct the contamination in Metlino during 1949–1956, a model of the site for this time period was also needed for Monte Carlo calculation.

The geometry of the historic model was created using two basic resources: A recently declassified hydrological map of this area (Fig. 5) and the water depth and activity measurements performed at the reservoir number 10. It was possible to overlay the historic map with the transects of the measurements and in this way to confirm the identification of the beds of the Techa River and the location of the central peninsula between the two river arms. Both these observations indicate

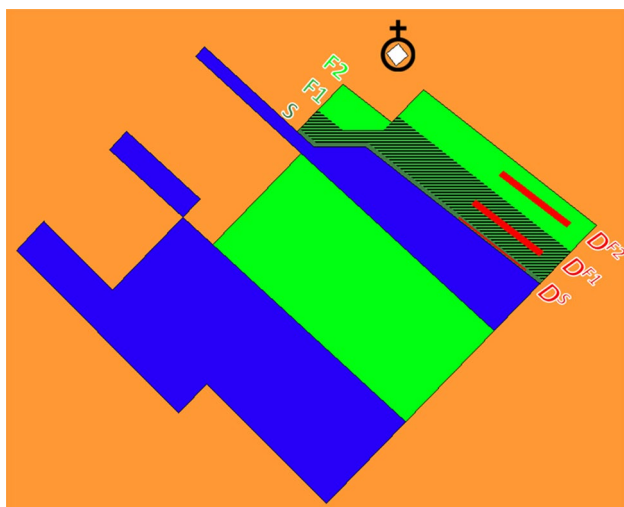


Fig. 15 Drawing of the historic Metlino model. Soil is shown in orange, the two arms of the Techa River coming out of the Metlinsky pond are shown in blue. On the upper left side, the river arms are limited by the dam. The church is in the central top location of the image. Areas acting as sources are indicated in green. The shoreline source S and the floodplain sources F_1 and F_2 are shown in dark green, shaded green, and light green, respectively. The detectors introduced over the shoreline (D^S) and over the floodplain D^{F_1}, D^{F_2} are shown in red. (Color figure online)

that the peninsula was sufficiently elevated in the top part to not have been flooded with contaminated water, but that the bottom part was frequently flooded and is, therefore, contaminated. In addition, on the other side of the river, towards the church, a possible floodplain was identified by determining plausible areas in the historic map. These areas were implemented as sources into the model (Fig. 15).

There are no measurements of the depth distribution of ^{137}Cs in soil in Metlino for the time period of 1949–1956. Therefore, Eq. (3) was used for estimation. Only 1 year after the contamination, most of the activity is in the first 2 cm of the soil; in contrast, for times up to 10 years after the contamination, the activity is distributed over 10 cm depth. Metlino was evacuated 7 years after the first contamination and repeatedly contaminated in these 7 years. Therefore, a standard depth of the activity distribution of 5 cm with minimal and maximal values of 2 and 10 cm was assumed. This approach was also used in Taranenko et al. 2003.

To consider the dependence of the dose rate on the distance to the shoreline measured in the 1950s (Fig. 10), the source area from the Techa River shore towards the church tower was divided into three sections: Shoreline (S), 0–1 m from the shore, Floodplain 1 (F_1), 1–10 m, and Floodplain 2 (F_2), 10–20 m distant from the shoreline.

Detectors 1 m above the ground were introduced in the simulation over all three sections at a far distance from the church, to account for the reference point of the 1950s measurements, being some 100 m away from the church. Each of the detectors scored the dose due to the different sources, D_x^y , with x denoting the detector and y the source (S, F_1, F_2). The relative source strengths, v_1 and v_2 , of the floodplain sources compared to the shoreline source were then calculated from:

$$R_1 = \frac{D_S^S + v_1 D_S^{F_1} + v_2 D_S^{F_2}}{D_{F_1}^S + v_1 D_{F_1}^{F_1} + v_2 D_{F_1}^{F_2}}, \quad R_2 = \frac{D_S^S + v_1 D_S^{F_1} + v_2 D_S^{F_2}}{D_{F_2}^S + v_1 D_{F_2}^{F_1} + v_2 D_{F_2}^{F_2}} \tag{10}$$

where $R_{1,2}$ are the relative dose ratios between shoreline and the respective floodplain, as explained above.

For the Metlino model, a dose conversion factor (DCF_j) between the dose per source particle in brick and the dose per source particle in air at the shoreline detector S can be calculated. The DCF_j depends on the selection of the brick detector j , because a different dose per particle is registered at different locations on the church tower.

$$DCF_j = \frac{D_{pp}(j)}{D_{pp}(S)} \tag{11}$$

Having calculated the dose in brick $D_{X,j}$ for the time of the contamination (1949–1956) using Eq. (9), the air kerma at the shoreline $K_{\text{Air},j}$ was calculated by dividing the dose in brick by the dose conversion factor:

$$K_{Air,j} = \frac{D_{X,j}}{DCF_j} \tag{12}$$

Uncertainty assessment

All measurements with their respective uncertainty were included in a Matlab program (The MathWorks Inc., Natick, MA, USA) where an uncertainty analysis was carried out using a Monte Carlo approach and assuming normally distributed uncertainties. A 95% confidence interval is calculated for the results. In addition, a triangular distribution for the most probable source depth of 5 cm for the Metlino model, a minimal source depth of 2 cm, and a maximal source depth of 10 cm was included in the calculation.

Results

Calculations using the reservoir model

Reconstruction of the current annual dose

The activity of the sources A_1 – A_{11} , derived using the reservoir model, is shown in Table 3. Sources 1–8 are in soil and have source strength in the order of 10^7 Bq m^{-2} , while source 9 is covered with an increasing amount of water with increasing distance from the church tower and has a source strength of 2.2×10^8 Bq m^{-2} . Sources 10 and 11 are covered by 2 m of water and have thus much higher source strength in the order of 10^9 – 10^{10} Bq m^{-2} .

Using these activities, the annual dose at the sampling sites was calculated and compared to the annual dose in

Table 3 Specific activity of the 11 source sections in the reservoir model

Source	Activity (10^8 Bq m^{-2}) [95% CI]
1	0.54 [0.39–0.73]
2	0.32 [0.26–0.40]
3	0.09 [0.06–0.12]
4	0.22 [0.17–0.29]
5	0.09 [0.07–0.13]
6	0.03 [0.02–0.04]
7	0.23 [0.16–0.31]
8	0.51 [0.38–0.68]
9	2.21 [1.65–2.95]
10	114.20 [44.23–191.15]
11	34.99 [9.01–63.93]

Sources 10 and 11 are shielded by water and have thus much higher source strength than sources 1–9

CI confidence interval

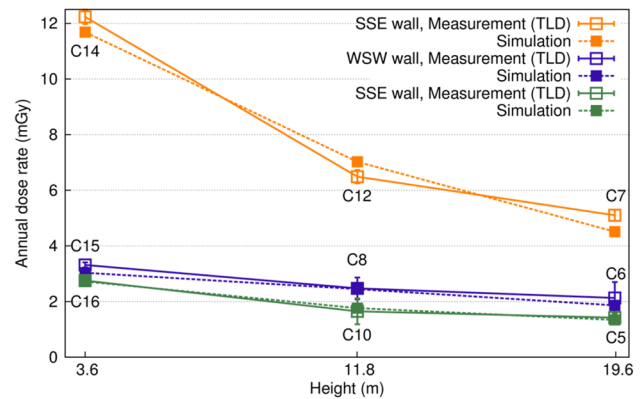


Fig. 16 Current annual doses measured using TLD compared to those simulated using the reservoir model

brick, converted from the TLD measurements, \hat{D}_j^{2012} . The simulated results are in good agreement with the measurements (Fig. 16). The NNW wall shows a steeper dose profile with the height of the wall than the walls facing towards WSW and SSE. The profile based on the measurements can only be reconstructed from the model when sources 10 and 11 are employed (see above).

Calculation of the anthropogenic dose in brick

As a first step, a dose in brick for the time after the evacuation (1956–2012), $D_{X,j}^{Reservoir}$, was calculated according to Eq. 8. The results show brick doses between 100–2000 mGy (Fig. 17). The simulations are in good agreement with estimations based on measurements only. For samples C1 and C9, no TLD measurements are available, and the reconstruction for those samples is based only on the estimations of the model. In general, the large uncertainty of the effective half-life T_{eff} leads to large uncertainties in its derived quantity $D_{X,j}^{Reservoir}$.

As second step, the anthropogenic dose in brick for the time before the evacuation (1949–1956), $D_{X,j}$, was calculated using the total dose in brick from the measurements, $D_{X,j}^{Total}$ according to Eq. 9 (Fig. 18). Due to the large uncertainty in $D_{X,j}^{Reservoir}$, resulting from the uncertainty in T_{eff} , no meaningful result for the anthropogenic brick dose $D_{X,j}$ is obtained. An alternative and possibly more precise derivation of the effective half-life seems possible when considering the following three points:

1. From Figs. 3 and 5, it is reasonable to assume that the area north to the church (housing area in the historic Metlino) was not contaminated.

Fig. 17 Dose in brick for the time after the evacuation (1956–2012). Doses are in the range of 100–2000 mGy. The x-axis shows the samples ordered by wall

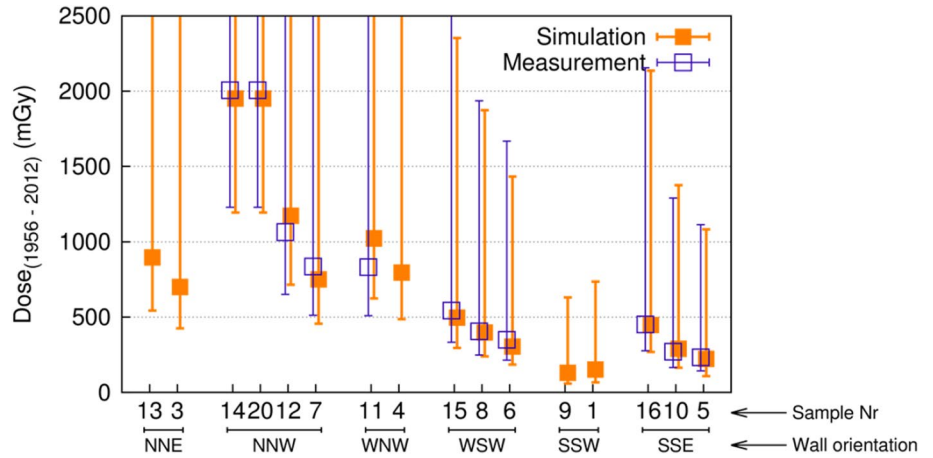


Fig. 18 Anthropogenic dose in brick for the time from 1949 to 1956. The x-axis shows the samples ordered by wall. Two dose values are shown per sample, calculated using two differently derived values for the effective half-life

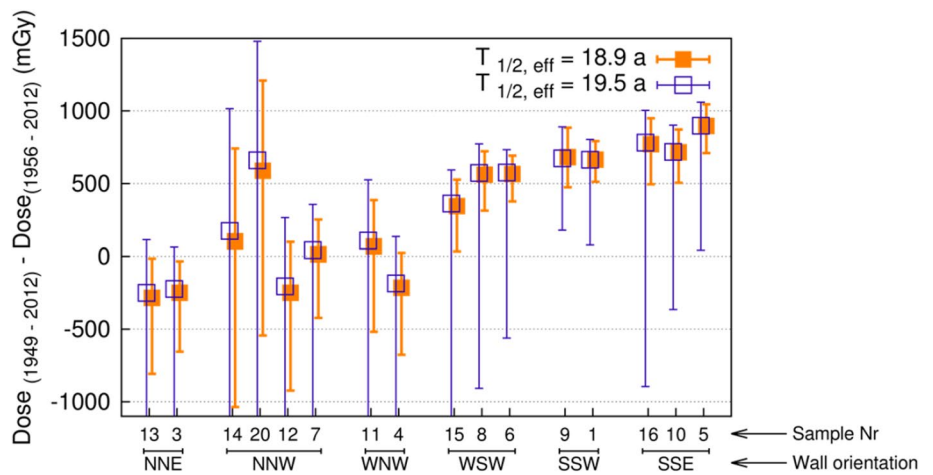


Table 4 Effective half-life of ^{137}Cs as determined from samples at the NNW wall of the church tower that were not exposed to anthropogenic radiation before the evacuation of Metlino

Wall	Height (m)	Sample	Effective half-life (a)
NNW	3.6	C14	18.3
	3.6	C20	16.0
	11.8	C12	20.6
	19.6	C7	19.9
Average			18.7 ± 2.0

2. The relative height profile for the NNW wall is the same for the TLD (dose rate today) and bricks (integrated dose rate from 1949 to today). This is a strong indication that the exposure geometry for this wall did not change and was the same as today, as opposed to the WSW and SSE walls, where the height profiles for brick and TLD are different.

3. The dose values in bricks for the time before evacuation for the samples from the NNW are compatible with zero dose and the best estimates are distributed around the zero dose value.

It thus seems reasonable to assume that the anthropogenic doses in the samples of the NNW wall were accumulated entirely in the time period after evacuation and installment of the reservoir, which created new sources. This, in turn, opens the possibility to use Eq. (8) for these samples to determine the effective half-life by back calculation, equating the $D_{Xj}^{\text{Reservoir}}$ with the measured D_{Xj}^{Total} . In this way, the effective half-life was determined for four different samples, and was averaged to be $T_{\text{eff}} = 18.7 \pm 2.0$ a (Table 4).

Using this value of the effective half-life leads to doses significantly different from zero (values shown in orange in Fig. 18). The samples facing towards the Techa River, at the WSW and SSE wall, received doses between 0.3 and 0.9 Gy. In contrast, all the samples facing away from the Techa River, at the NNW wall, did not receive a dose significantly

different from zero in the time before the evacuation. Obviously, all doses on the NNW wall were accumulated after the evacuation.

Calculations using the historic Metlino model

Dose ratio between WSW and SSE walls

Having sampled two walls facing towards the Techa River, the NNW and WSW wall, it is possible to calculate the ratio of the samples on the NNW wall to the matching sample of the WSW wall. This ratio can be calculated using the doses measured in brick or based on calculations using the historic Metlino model. A comparison of these two results can be used to verify the scenario created for the historic Metlino. As it can be seen in Fig. 19, the ratio between the doses is about 1 for the historic Metlino model but only about 0.6 for the measurements of the reservoir model.

Depth-dose distribution in bricks

For most brick samples, the dose was estimated at a depth of 1 cm from the surface of the brick. For samples C5 and C6, the dose was also determined at depth of 3, 5, and 7 cm, for C5, additionally, at 9 cm. This allowed for the determination of depth distribution of the dose in the brick.

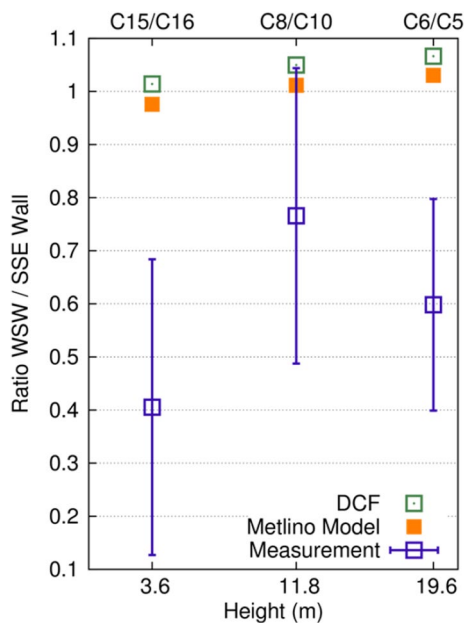


Fig. 19 Ratio of the dose in brick for the time before the evacuation (1949–1956) between samples of equal height in the WSW and the SSE wall. For estimations of the dose based on measurements, the ratio is between 0.4 and 0.8. Calculations based on the simulations show an equal dose on both walls. DCF means dose conversion factor between doses in bricks and doses at the shoreline, estimated with the Metlino model, see “Results” section

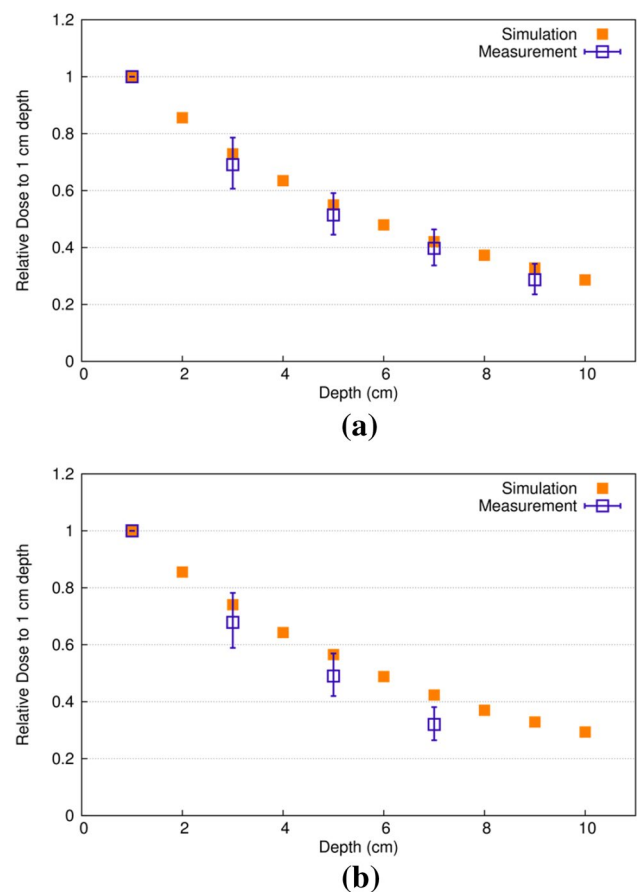


Fig. 20 Depth-dose distribution in brick for time before the evacuation of Metlino (1949–1956); **a** sample C5, SSE wall, top position. **b** sample C6, WSW wall, top position

The measured dose in brick, D_{Xj}^{Total} , is the total dose accumulated during the inhabitation of Metlino and after the evacuation. For a comparison with the Monte Carlo calculations of the historic Metlino model, the measured dose-depth profiles need to be corrected for the reservoir dose. This was done using the calculation of the reservoir model to obtain present-day dose rates for all depth intervals analyzed of samples C5 and C6. Depth-dependent reservoir doses were then calculated using Eq. (8) and subtracted from the measured doses (Fig. 20). Calculations based on the historic Metlino model resulted in the same rate of a decreasing dose with the depth in the brick as the calculations based on measurements (Fig. 20).

ICRU Report 68 (2002) suggests that the dose-depth profile gives information about the source energy, but that the profile is also dependent, to some extent, on the source configuration. While the dose height profile is a more sensitive indicator of the latter, the dose-depth profile in Fig. 20 does overall confirm the assumed source configuration and energy in this study.

Air kerma at shoreline

For the calculation of the air kerma at the shoreline, the source distribution at the shoreline and the floodplain has to be determined. The measurements of the sediment activity suggest a relatively homogeneous, constant contamination of the floodplain on the peninsula, between the two main arms of the Techa River (see Figs. 5, 6), which is also implemented in the model.

With this source configuration implemented in the historic Metlino model, the doses per source particle in the shoreline detector $D_{pp}(S)$ and the brick detector j , $D_{pp}(j)$, were calculated. Table 5 shows the DCF_j for the six different samples at the WSW and SSE walls as well as for two samples on the south-southwestern (SSW) wall (only in the octagonal stories).

The calculation showed that the results vary depending on whether brick doses from the WSW and SSW wall or SSE wall were used (Fig. 21; Table 6). For the WSW wall, an average air kerma of 27.7 Gy, for the SSW wall of 22.4 Gy, and for the SSE wall of 48.0 Gy is obtained.

Table 5 Dose conversion factors between a dose at the shoreline of the Techa River and the samples at the church tower, calculated with the historic Metlino model

Wall	Height (m)	Sample	DCF
WSW	3.6	C15	0.0144
	11.8	C8	0.0190
	19.6	C6	0.0193
SSW	11.8	C9	0.0302
	19.6	C1	0.0302
SSE	3.6	C16	0.0142
	11.8	C10	0.0181
	19.6	C5	0.0181

Fig. 21 Time integrated air kerma at shoreline for the time between 1949 and 1956 for the samples on the WSW, SSW, and SSE walls. The integral air kerma values are averaged separately for samples of each wall and given with the respective 95% confidence interval. The dose conversion factor (DCF) for each sample is also shown

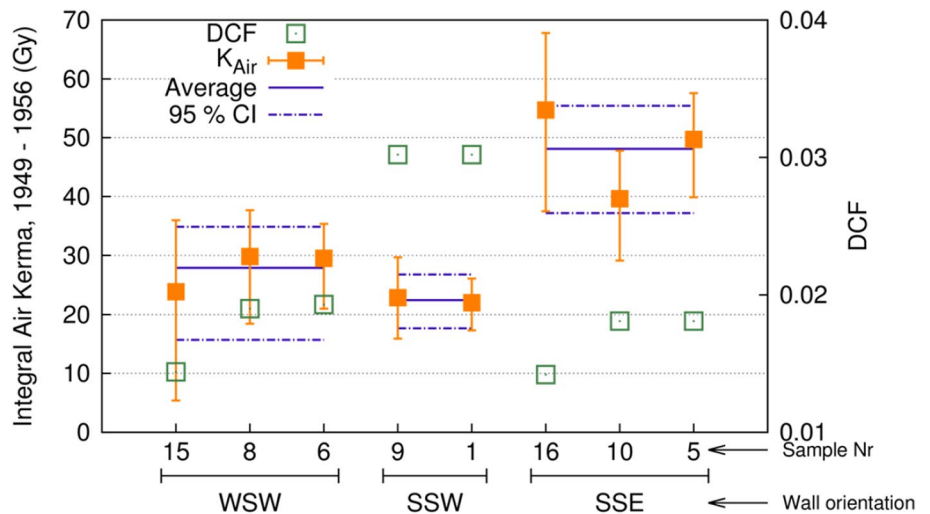


Table 6 Air kerma at shoreline of the historic Metlino model calculated based on the results from the sampling locations on the church tower

Wall	Height (m)	Sample	K_{air} (Gy) [95% CI]
WSW	3.6	C15	23.9 [5.4–36.0]
	11.8	C8	29.8 [18.4–37.7]
	19.6	C6	29.5 [21.0–35.4]
		Average	27.7 [14.9–36.3]
SSW	11.8	C9	22.9 [15.9–29.7]
	19.6	C1	22.0 [17.3–26.1]
		Average	22.4 [16.6–27.9]
SSE	3.6	C16	54.7 [37.5–67.8]
	11.8	C10	39.6 [29.1–47.8]
	19.6	C5	49.7 [39.9–57.6]
		Average	48.0 [35.5–57.7]
Average WSW and SSW samples			25.6 [15.6–33.0]

CI confidence interval

Discussion

The experimental information gathered in this study includes measured TLD brick doses and annual TLD doses. The uncertainties associated with these measurements were quantified and considered in the calculations. For a detailed discussion on the TL/OSL measurements, the reader is referred to Woda et al. (in prep.). In contrast, the estimation of the air kerma at the shoreline by radiation transport calculations is based on the assumption of a specific exposure geometry in the model, which includes a certain degree of subjectivity. In the current study, this estimation suffers from incomplete knowledge and data, which results in a systematic uncertainty that is difficult to quantify in such a complex system.

Measurement uncertainties and assumptions

The largest (quantifiable) uncertainty in this work is due to the determination of the effective half-life of ^{137}Cs . The initial approach to estimate the effective half-life was to use measurements of the specific activity of ^{137}Cs in water over the last 60 years. This approach is based on the assumption that there is a dynamic equilibrium between the activity of ^{137}Cs in water and bottom sediment (and/or soil), so that the former can be used as a proxy for the latter (Taranenko et al. 2003). However, it was found that the effective half-life determined with this method is associated with a large uncertainty, which leads to numerical values for the effective half-life that are not significantly different from zero, and thus are not meaningful. Measurements of the current dose rate as with TLD along the height of the NNW wall church tower, and an analysis of the terrain elevation suggest that the swampy part to the north-west of the church tower was clean when Metlino was inhabited, and only post-contaminated by infiltrated reservoir water after the creation of reservoir number 10. With this assumption, it was possible to use the samples from the NNW wall to estimate the effective half-life with greater precision.

Measurements on the reservoir 10 helped to reconstruct the geometry and source configuration for the historic Metlino model. The ground level of the reservoir number 10 shows the elevation profile of Metlino (Fig. 6). The activity measurement of the bottom sediment of Reservoir 10 indicates that the contamination was caused by the contaminated Techa River before the creation of the reservoir; contaminated debris is expected on both sides of the river, deposited in times of high water levels.

The two main sources of uncertainty in producing the overlay of the map and the transects are: (a) The alignment of the transects measured on the boat over the current map; this could only be done as a best estimate as there are no GPS or other landmark data available. (b) The combination of these transects with the historic map; it is difficult to assess the exact starting point of the boat towards the church. It is believed, however, that the overlay shown in Fig. 5 gives the best estimation possible.

In addition, environmental factors that hardly can be quantified play a role, like the influence of weather and rainfall to the water levels. The area of former Metlino is widely covered by the large Reservoir 10 that shields the previous contaminated areas. On its shores, however, it builds up large swampy areas. Depending on weather conditions and rainfall throughout the year, those areas might be covered with a considerable amount of water in rainy years shielding the contaminated ground below. In years with low precipitation, the marsh lands may dry out, exposing the contaminated soil to the environment, causing contamination in the surrounding. The All-Russia Research

Institute of Hydrometeorological Information-World Data Center (RIHMI-WDC) database for the location of Ekaterinburg (about 200 km away from Metlino) shows strong variations of the annual rainfall. Looking at the dose rate mapping measurements (Fig. 7), a difference in the dose rate measured in 2012 and in 2013 can be seen. Using TLD that remained in the church tower for 1 year (instead of performing a single snapshot like dose rate measurement that averages only over a few minutes on one specific day) was a means to average variations in the daily precipitation levels. The TLD give a year average that is much more reliable than a single measurement. However, it is not clear whether the year 2012 is representative for the last 60 years after the evacuation.

Model uncertainties

The main uncertainty in the historic Metlino model is driven by the geometry of the landscape around the church tower and the determination of contaminated areas.

The present measurements on the bottom of reservoir number 10 and the analysis of the historic map indicate that the path of the Techa River through the former village of Metlino, and thus, the contaminated areas at its shore, were different than assumed in the previous studies. From the present work, there is no evidence to support the assumption by Mokrov, 2004, that the main sources of the radiation exposure in Metlino were due to the contamination of the Metlinsky pond. In contrast, the findings presented here show that a shoreline and floodplain source of the Techa River downstream of the Metlinsky pond is necessary to explain the measured brick doses.

Figure 19 shows the dose ratio of brick samples between the WSW and the SSE wall for the time before the evacuation. The comparison, which is based on measurements, shows ratios of 0.4–0.8 between the walls, while the comparison based on simulations using the historic Metlino model shows an equal dose in both walls. This suggests that the actual historic source is distributed in a way that results in more doses to the SSE wall, while the source used for the simulation has a similar contamination in the vicinity of the two walls. With the limited number of documents available that describe the situation in Metlino, it was not possible to reconstruct a more detailed source in the vicinity of the church tower than the one presented here. Any change to the configuration of the models used for the Monte Carlo calculations with the implication of reconstructing the dose ratio between the walls as seen from the measurements would not be justifiable.

Historic measurements indicate that the level of contamination was higher for the shoreline than for the floodplain, yet they do not provide any information about the size of

Table 7 Comparison of the integral air kerma at the Techa shoreline derived from luminescence studies of bricks in Metlino and Muslyumovo and those assumed in the Techa River Dosimetry System (TRDS) (version of 2016)

Location, time period	Building, wall orientation		Air kerma (Gy) [95% CI]	
			Estimated from doses in brick	Assumed in TRDS-2016
Metlino, 7 km from release site, 1949–1956	Mill	SW ^b	23 [15–32]	21 [11–42]
		Church	28 [15–36]	
	SSW ^a	22 [17–28]		
	SSE ^a	48 [36–58]		
Muslyumovo, 78 km from release site, 1949–2007	Mill	W ^c	2.2 [0.2–1.5]	1.9 [0.9–3.8]

CI confidence interval

^aThis work

^bAccording to Taranenko et al. (2013)

^cAccording to Ulanovsky et al. (2009)

the shoreline area. The width of 1 m for the contaminated shoreline in Eq. (10) is somewhat arbitrary and chosen in accordance with Taranenko et al. (2003). However, whatever value is chosen for the width of the shoreline, it will always be an over-simplification of the real geometry and the contamination pattern that today cannot be accurately reconstructed anymore.

To investigate the influence of a highly contaminated shoreline on the dose ratio of samples from the SWS to the SSE wall, a sensitivity analysis was carried out. It was found that the dose ratio in the historic Metlino geometry could only be reproduced if a very high contamination of a 100-fold excess relative strength at source areas further downstream from the church tower was assumed. However, such an approach would result in an unrealistically high air kerma value of about 100 Gy.

Comparison with other studies and the TRDS evaluation

Table 7 summarizes the results of the present study compared to the results of the earlier luminescence studies performed in the Techa River region (Taranenko et al. 2013; Ulanovsky et al. 2009) as well as to the evaluation of the integral air kerma derived from the values of dose rate at the river shoreline assumed in the Techa River Dosimetry System (version of 2016) (Degteva et al. 2017).

As can be seen from Table 7, the integral air kerma above the shoreline in Metlino (located 7 km from the release site) calculated earlier from the measured doses in bricks of the SW wall of the mill (Taranenko et al. 2013) is in agreement with the results of the present study for the WSW and SSW walls of the church tower (23 vs. 28 and 22 Gy). The present estimates are also in good agreement with the TRDS-assumed value, 21 [11–42] Gy (95% confidence interval). The estimate obtained from the SSE wall

of the church tower (48 [36–58] Gy), however, is significantly higher than the other estimates, but still agrees with the TRDS-assumed value within the given confidence limits. A possible reason for the dose difference in both walls of the church tower (see Fig. 19) could be a higher contamination of more distant sources, located at the downstream end of the Metlino residence area, compared to sources closer to the church.

Table 7 also shows that the integral air kerma above the shoreline in Muslyumovo, calculated by Ulanovsky et al. (2009) from the measured doses in bricks of the western wall of the mill (2.2 Gy), is ten times lower than that in Metlino. This is because Muslyumovo was located much farther from the source of radioactive discharge (78 km from the release site). The estimate calculated by Ulanovsky et al. (2009) is also in good agreement with the TRDS-assumed value for Muslyumovo equal to 1.9 Gy (Table 7).

Conclusions and outlook

From the brick samples of the three walls of the church tower (WSW, SSW, and SSE) time integrated air kerma values at the shoreline from 1949 to 1956 were estimated, that are in parts significantly different, with the best estimates differing by more than a factor of two (23–46 Gy). However, all air kerma values agree with the value adopted in the TRDS-2016, within the respective uncertainty ranges. Given the complexity of the reconstruction and the high degree of incomplete knowledge of the exact exposure geometry for the historic period, especially for the area facing the SSE wall, the experimental, and modelling results can be regarded as an overall validation of the external doses predicted by TRDS-2016.

Nevertheless, it would be desirable in future studies to map the sediment activity over the entire area of interest, not only in the vicinity of the church tower but also further down the former riverbed, close to the simulated air detectors shown in Fig. 14. Moreover, measurements should be performed along more than just the four transects used in this study. With a more detailed picture of the radiological situation, a more accurate evaluation study—especially with regard to the dose information stored in the SSE wall of the church tower—should be feasible.

Furthermore, it remains to be resolved if the situation at the reference point, with a drop in the dose rate, and the contamination of more than one order of magnitude in the first 20 m from the shoreline is representative all along the shoreline, or only a local phenomenon. Results of the few sediment activity measurements in the area close to the church indicate a more homogeneous contamination in this area as compared to the reference point (Figs. 5, 6). This would imply a more complex source configuration than was assumed in the present study. If so, this configuration could be included in future updates of the TRDS.

Acknowledgements This study has received funding from the European Community's Seventh Framework Program (FP7/2007–2013) under Grant Agreement No. 249675. Financial support for Mauritius Hiller to prepare this manuscript and publish these data was provided by the Russian Health Studies Program of the U.S. Department of Energy (DOE) under the auspices of the Joint Coordinating Committee for Radiation Effects Research Project 1.1, Techa River Population Dosimetry.

References

- Anspaugh LR, Degteva MO, Vasilenko EK (2002) Mayak production association: introduction. *Radiat Environ Biophys* 41:19–22
- Bougrov NG, Göksu HY, Haskell E, Degteva MO, Meckbach R, Jacob P (1998) Issues in the reconstruction of environmental doses on the basis of thermoluminescence measurements in the Techa Riverside. *Health Phys* 75:574–583
- Bougrov N, Baturin A, Göksu Y, Degteva O, Jacob P (2002) Investigations of thermoluminescence dosimetry in the Techa River Flood Plain: analysis of the new results. *Radiat Prot Dosim* 101:225–228
- Davis FG, Krestinina LY, Preston D, Epifanova S, Degteva M, Akleyev AV (2015) Solid cancer incidence in the Techa River Incidence Cohort: 1956–2007. *Radiat Res* 184:56–65
- Degteva MO, Kozheurov VP, Tolstykh EI, Vorobiova MI, Anspaugh LR, Napier BA, Kovtun AN (2000a) The Techa River dosimetry system: methods for the reconstruction of internal dose. *Health Phys* 79(1):24–35
- Degteva MO, Vorobiova MI, Kozheurov VP, Tolstykh EI, Anspaugh LR, Napier BA (2000b) Dose reconstruction system for the exposed population living along the Techa River. *Health Phys* 78(5):542–554
- Degteva MO, Vorobiova MI, Tolstykh EI, Shagina NB, Shishkina EA, Anspaugh LR, Napier BA, Bougrov NG, Shved VA, Tokareva EE (2006) Development of an improved dose reconstruction system for the Techa River population affected by the operation of the Mayak Production Association. *Radiat Res* 166:255–270
- Degteva MO, Bougrov NG, Vorobiova MI, Jacob P, Göksu H (2008) Evaluation of anthropogenic dose distribution amongst building walls at the Metlino area of the upper Techa River region. *Radiat Environ Biophys* 47:469–479
- Degteva MO, Shagina NB, Vorobiova MI, Anspaugh LR, Napier BA (2012) Reevaluation of waterborne releases of radioactive materials from the Mayak Production Association into the Techa River in 1949–1951. *Health Phys* 102(1):25–38
- Degteva MO, Shagina NB, Shishkina EA, Vozilova AV, Volchkova AY, Vorobiova MI, Wieser A, Fattibene P, Della Monaca S, Ainsbury E, Moquet J, Anspaugh LR, Napier BA (2015a) a) Analysis of EPR and FISH studies of radiation doses in persons who lived in the upper reaches of the Techa River. *Radiat Environ Biophys* 54:433–444
- Degteva MO, Vasilenko EK, Wieser A, Woda C, Fattibene P, Ainsbury EA (2015b) Dose reconstruction in the SOLO project for Mayak workers and former residents of the Techa River area. Abstracts of the 7th international MELODI workshop “Next generation radiation protection research”, Munich, p 57
- Degteva MO, Shishkina EA, Tolstykh EI, Vozilova AV, Shagina NB, Volchkova AY, Ivanov DV, Zalyapin VI, Akleyev AV (2017) Application of the EPR and FISH methods to dose reconstruction for people exposed in the Techa River area. *Radiat Biol Radioecol* 57:30–41 (in Russian)
- Eckerman KF, Ryman JC (1993) Federal Guidance Report 12—external exposure to radionuclides in air, water, and soil. Staff Report of the Federal Radiation Council
- Göksu HY, Degteva MO, Bougrov NG, Meckbach R, Haskell EH, Bailiff IK, Bøtter-Jensen L, Jungner H, Jacob P (2002) First international intercomparison of luminescence techniques using samples from the Techa River Valley. *Health Phys* 82:94–102
- ICRU Report 68 (2002) Retrospective assessment of exposures to ionising radiation. International Commission on Radiation Units and Measurements. *J. I.C.R.U.* 2 (No. 2)
- Ivanov O, Danilovich A, Potapov V, Stepanov V, Smirnov S, Volkovich A (2013) Peculiarities of environment pollution as a special type of radioactive waste: field means for comprehensive characterization of soil and bottom sediments and their application in the Survey at the Floodplain of Techa River. In: WM2013 Conference, Phoenix
- Jacob P, Gering F, Meckbach R (1997) Kerma rates in air several years after a ¹³⁷Cs deposition. *Kerntechnik* 62(2–3):99–103
- Jacob P, Göksu Y, Taranenko V, Meckbach R, Bougrov NG, Degteva MO, Vorobiova MI (2003) On an evaluation of external dose values in the Techa River Dosimetry System (TRDS) 2000. *Radiat Environ Biophys* 42:169–174
- Jacob P, Fesenko S, Bogdevitch I, Kashparov V, Sanzharova N, Grebenshikova N, Isamov N, Lazarev N, Panov A, Ulanovsky A, Zhuchenko Y, Zhurba M (2009) Rural areas affected by the Chernobyl accident: radiation exposure and remediation strategies. *Sci Total Environ* 408(1):14–25
- Karsten R (1997) *Bauchemie—Handbuch für Studium und Praxis*, 10th edn. C.F. Müller, Heidelberg
- Krestinina LY, Davis FG, Schonfeld S, Preston DL, Degteva M, Epifanova S, Akleyev AV (2013a) Leukemia incidence in the Techa River Cohort: 1953–2007. *Br J Cancer* 109:2886–2893
- Krestinina LY, Epifanova S, Silkin S, Mikryukova L, Degteva M, Shagina N, Akleyev A (2013b) Chronic low-dose exposure in the Techa River Cohort: risk of mortality from circulatory diseases. *Radiat Environ Biophys* 52:47–57
- Minenko VF, Ulanovsky AV, Drozdovitch VV, Shemiakina EV, Gavrilin YI, Khrouch VT, Shinkarev SM, Voillequé PG, Bouville A, Anspaugh LR, Luckyanov N (2006) Individual thyroid

- dose estimates for a case-control study of Chernobyl-related thyroid cancer among children of Belarus—part II. Contributions from long-lived radionuclides and external radiation. *Health Phys* 90(4):312–327
- Mokrov YG (2004) External radiation exposure of residents living close to the Mayak facility: main sources, dose estimates, and comparison with earlier assessments. *Radiat Environ Biophys* 43(2):127–139
- Mokrov YG, Glagolenko, Napier B (2000) Reconstruction of the radionuclide contamination of the Techa River caused by liquid waste discharge from radiochemical production at the Mayak Production Association. *Health Phys* 79(1):15–23
- Mokrov YG, Stukalov PM, Martyushov VZ (2005) On the problem of external exposure dose estimation for Metlino residents (Techa River, Chelyabinsk region) in the early 1950s. *Radiat Saf Probl* 4:51–57 (in Russian)
- Potapov V, Danilovich A, Ignatov S, Volkovich A, Ivanov O, Stepanov V, Volkov V (2006) Non-destructive measurements of the characteristics of radioactive contamination of near surface layers of concrete and ground with collimated spectrometric detectors WM'06 conference, Tucson
- Schonfeld S, Krestinina L, Epifanova S, Degteva M, Akleyev A, Preston D (2013) Solid cancer mortality in the Techa river cohort (1950–2007). *Radiat Res* 179:183–189
- Shagina NB, Vorobiova MI, Degteva MO, Peremyslova LM, Shishkina EA, Anspaugh LR, Napier BA (2012) Reconstruction of the contamination of the Techa River in 1949–1951 as a result of releases from the “MAYAK” Production Association. *Radiat Environ Biophys* 51:349–366
- Shishkina EA, Volchkova AY, Timofeev YS, Fattibene P, Wieser A, Ivanov DV, Krivoschapov VA, Zalyapin VI, Della Monaca S, De Coste V, Degteva MO, Anspaugh LR (2016) External dose reconstruction in tooth enamel of Techa riverside residents. *Radiat Environ Biophys* 55(4):477–499
- Taranenko V, Meckbach R, Degteva MO, Bougrov NG, Göksu Y, Vorobiova MI, Jacob P (2003) Verification of external exposure assessment for the upper Techa riverside by luminescence measurements and Monte Carlo photon transport modeling. *Radiat Environ Biophys* 42(1):17–26
- Taranenko VA, Vorobiova MI, Degteva MO, Bougrov NG, Cherepanova EI, Kuropatenko ES (2013) Verification of the external exposure levels in the upper streams of Techa River (Metlino) by luminescence measurements. *Med Radiol Radiat Saf* 58(1):29–35 (in Russian)
- X-5 Monte Carlo Team (2008) MCNP—a general Monte Carlo N-particle transport code, Version 5, LA-UR-03-1987
- Ulanovsky A, Woda C, Jacob P, Bougrov N (2009) Advanced validation of population external exposures in radioactively contaminated Techa River Valley. In: Late health effects of ionizing radiation: bridging the experimental and epidemiologic divide conference, Washington DC, National Cancer Institute, Bethesda, p 101
- Ulanovsky A, Woda C, Jacob P, Bougrov N, Degteva M, Ivanov O (2010) Advanced validation of the TRDS external dose estimates in Muslymovo with luminescences measurements. SOUL meeting
- Vorobiova MI, Degteva MO, Burmistrov DS, Safronova NG, Kozheurov VP, Anspaugh LR, Napier BA (1999) Review of historical monitoring data on Techa River contamination. *Health Phys* 76(6):605–618
- Vozilova AV, Shagina NB, Degteva MO, Edwards AA, Ainsbury EA, Moquet JE, Hone P, Lloyd DC, Fomina JN, Darroudi F (2012) Preliminary FISH-based assessment of external dose for residents exposed on the Techa River. *Radiat Res* 177:84–91
- Woda C, Jacob P, Ulanovsky A, Fiedler I, Mokrov Y, Rovny S (2009) Evaluation of external exposures of the population of Ozyorsk, Russia, with luminescence measurements of bricks. *Radiat Environ Biophys* 48(4):405–417
- Woda C, Ulanovsky A, Bougrov NG, Fiedler I, Degteva MO, Jacob P (2011) Luminescence dosimetry in a contaminated settlement of the Techa River valley, Southern Urals, Russia. *Radiat Meas* 46(3):277–285